Nuclear export of the influenza virus ribonucleoprotein complex: Interaction of Hsc70 with viral proteins M1 and NS2

Ken Watanabe [a], Teppei Shimizu [a], Saiko Noda [a], Fujiko Tsukahara [b], Yoshiro Maru [b], Nobuyuki Kobayashi [a,c,*]

[a] Laboratory of Molecular Biology of Infectious Agents, Graduate School of Biomedical Sciences, Nagasaki University, 1-14 Bunkyo-machi, Nagasaki 852-8521, Japan
[b] Department of Pharmacology, Tokyo Women's Medical University, School of Medicine, 8-1, Kawada-cho, Shinjuku-ku, Tokyo 162-8666, Japan
[c] Central Research Center, AVSS Corporation, 1-22, Wakaba-machi, Nagasaki 852-8137, Japan

ABSTRACT

The influenza virus replicates in the host cell nucleus, and the progeny viral ribonucleoprotein complex (vRNP) is exported to the cytoplasm prior to maturation. NS2 has a nuclear export signal that mediates the nuclear export of vRNP by the vRNP–M1–NS2 complex. We previously reported that the heat shock cognate 70 (Hsc70) protein binds to M1 protein and mediates vRNP export. However, the interactions among M1, NS2, and Hsc70 are poorly understood. In the present study, we demonstrate that Hsc70 interacts with M1 more strongly than with NS2 and competes with NS2 for M1 binding, suggesting an important role of Hsc70 in the nuclear export of vRNP.

© 2014 The Authors. Published by Elsevier B.V. on behalf of the Federation of European Biochemical Societies. This is an open access article under the CC BY-NC-ND license (http://creativecommons.org/licenses/by-nc-nd/3.0/).

1. Introduction

Influenza viruses are enveloped, negative-strand RNA viruses with segmented genomes, which belong to the family *Orthomyxoviridae*. Influenza pandemics or seasonal epidemics cause significant morbidity and mortality in humans and animals.

The influenza virus binds to sialic acids on the cell surface via hemagglutinin (HA) and is incorporated into the cell via endocytosis. The low pH within the endosome promotes the fusion of the viral membrane and endosome, which is accompanied by structural changes in HA [1]. Moreover, the H^+ influx from the endosome into the virion is mediated by the M2 protein. As a result, the viral ribonucleoprotein complex (vRNP) dissociates from M1 protein and releases into the cytoplasm. vRNP comprises viral RNA; NP; and the viral RNA polymerases PA, PB1, and PB2; and each vRNP protein contains a nuclear localization signal (NLS).

Thus, the cellular nuclear import factor, importin alpha, binds to NLS and imports vRNP into the nucleus via the nuclear pore complex. Further, replication and early transcription from vRNP occur in the nucleus, and the viral mRNAs are exported from the nucleus [2]. The newly synthesized viral proteins, i.e., NP, PB1, PB2, and PA, are imported into the nucleus via their NLS, and they form a complex with the newly synthesized viral RNA to form progeny vRNP [3]. The progeny vRNP is exported from the nucleus into the cytoplasm by the cellular nuclear export factor CRM1/exportin1-mediated pathway and then transported via microtubules to beneath the cellular membrane [4,5], following which, virus assembly occurs on the plasma membrane with the newly synthesized structural proteins such as M1, M2, HA, neuraminidase (NA), and NS2. The virus particles are then released from the cell via the activity of NA [6].

The mechanism for the nuclear export of vRNP was initially reported by Martin et al. [7]. M1 is essential for the nuclear export of the progeny vRNP because the inhibition of M1 synthesis by H-7 [8] and the microinjection of M1 antibody into infected cells results in the inhibition of the nuclear export of vRNP. CRM1/exportin1 mediates the nuclear export pathway [9]. CRM1 recognizes the leucine-rich nuclear export signal (NES) and nuclear export occurs under the regulation of Ran protein. NS2 has a

well-characterized functional NES (^{12}ILMRMSKMQL^{21}) [10], which is recognized by CRM1. Recent studies have also demonstrated the existence of additional NESs on NS2 [11], M1 [12], and NP [13]. In addition, other studies, including our own previous research, have shown that the nuclear export of vRNP is inhibited by leptomycin B (LMB) [14,15], which is an inhibitor of the NES–CRM1 interaction [16]. Biochemical analyses have shown that NS2 directly interacts with M1 [17–19]. Based on these observations, it was hypothesized that the nuclear export of vRNP is mediated by the vRNP–M1–NS2–CRM1 complex [20–22]. Thus, NS2 is designated as the nuclear export protein (NEP). However, other reports suggest that NS2 is not essential for the nuclear export of vRNP because it does not colocalize with vRNP [23], and viruses that contained mutations in the NES of NS2 could be recovered [10]. It has been speculated that NS2 is not essential for the nuclear export of vRNP–M1 complex. Therefore, we explored the new M1-binding factor, which is related to the nuclear export of vRNP, and found that the host heat shock cognate protein 70 (Hsc70), a constitutive form of Hsp70 family protein, can mediate the nuclear export of vRNP [24]. Hsc70 is involved in the cell entry of rotavirus [25], but little is known about the role of Hsc70 in the influenza virus replication cycle. The LMB-sensitive NES in Hsc70 (^{394}LDVTPLSL^{401}) has been identified [26], and it is likely that the nuclear export of vRNP is regulated by M1, NS2, and Hsc70 [27]. However, the interactions among M1, NS2, and Hsc70 are not yet well understood.

The present study examined the binding activity of Hsc70 and influenza viral NS2 protein with the viral M1 protein based on biochemical analyses. We found that Hsc70 binds to M1 via its peptide-binding domain. Furthermore, we characterized the dissociation constant (K_d) values of the Hsc70–M1 and NS2–M1 interactions. The interaction of Hsc70–M1 was stronger than that of NS2–M1, suggesting an important role of Hsc70 in the export of vRNP.

2. Materials and methods

2.1. Antibodies and vector

The anti-M1 antibody was prepared by a previously described method [24]. The anti-GST antibody and anti-His antibody were purchased from GE Healthcare and Santa Cruz, respectively. For the expression of GST–Hsc70 wild-type (1–646 aa), pGEX2T–Hsc70 [28] was used. For the expression of GST–fused Hsc70 deletion mutants encoding 1–384 aa (N384), 1–402 aa (N402), 385–646 aa (C385), and 403–646 aa (C403), DNA fragments were generated by PCR amplification (Table 1) from pEGFP–Hsc70 [26]. The resultant PCR fragments were digested with BamHI and inserted into the BamHI-digested site of pGEX2T. For the expression of GST–fused Hsc70 deletion mutants encoding 1–462 aa (N462) and 1–546 aa (N546), Hsc70 cDNA encoding 1–462 aa

and 1–546 aa were generated by PCR amplification (Table 1) and subcloned in-frame into BamHI site of pGEX2T.

2.2. Purification of recombinant His–M1, GST–NS2, and GST–Hsc70

His–M1 was purified in accordance with the pET-system manual (Novagen) and a previous study [17]. In brief, His–M1 expressed by Escherichia coli was sonicated in a binding buffer [5 mM imidazole, 0.1 M NaCl, 20 mM Tris–HCl (pH 7.9), and 1% CHAPS], and the purified His–M1 was immediately used for GST-pull-down assays. GST–NS2 [17] and GST–Hsc70 [28] were purified in accordance with the glutathione Sepharose 4B manual (GE Healthcare) with some modifications. In brief, E. coli that expressed GST-fused protein was sonicated in a NET/NP-40 buffer [50 mM Tris–HCl (pH 7.9), 0.1 M NaCl, 5 mM EDTA, and 0.1% NP-40], and the NET/NP-40 buffer was also used as the wash buffer.

2.3. Pull-down assays

For the GST pull-down assay, GST-fused protein bound to 10 μl (bed volume) of glutathione Sepharose 4B was incubated at 4 °C for 1 h with purified His–M1 in the NET/NP-40 buffer. The beads were then washed three times with the NET/NP-40 buffer at 4 °C. To detect the GST-fused protein and His–M1, a western blot analysis was performed using either anti-GST or anti-M1 antibody. For the His-tag pull-down assay, His–M1 bound to 10 μl (bed volume) of His-bind resin (Novagen) was incubated for 1 h at 4 °C with the purified GST-fused protein in the binding buffer. The beads were then washed three times with the binding buffer at 4 °C. Further, to detect the GST-fused protein and His–M1, a western blot analysis was performed using either anti-GST or anti-His antibody.

3. Results

3.1. Hsc70 peptide-binding domain mediates association with M1

To identify the M1 binding region of Hsc70, a far-western blotting assay was performed using Hsc70 deletion mutants (Fig. 1A). N384 (1–384 aa) contained the ATPase domain, N402 (1–402 aa) contained the ATPase domain and NES, and N462 contained the ATPase domain, NES, and the N-terminal half of the peptide-binding domain. In addition, N546 (1–546 aa) lacked the variable domain, and C385 (385–646 aa) contained the peptide-binding domain, NES, and the variable domain but lacked the ATPase domain. C403 (403–646 aa) contained most of the peptide-binding domain and the variable domain but lacked the ATPase domain and NES. The GST-fused deletion mutants were expressed in E. coli. After purification, we confirmed the quality of the purified GST-fused proteins (Fig. 1B). His–M1 was expressed by E. coli and the lysate was reacted on a PVDF membrane with the purified GST–Hsc70 mutants. The far-western blotting performed with the GST–Hsc70 wild-type detected strong binding to M1. No signals were detected without the probe ["(−)"] or GST alone. The strongest signal was detected when the N462 mutant was used as a probe. Only weak signals were detected with N384 and C403, which lacked the NES sequence (Fig. 1C). The results shown in Fig. 1C were quantified using Image J software (Fig. 1D and Table 2). These results suggest that the N-terminal half of the peptide-binding domain (385–462 aa) of Hsc70 is essential for M1 binding.

3.2. C-terminal half of M1 is required for binding to Hsc70

To confirm the Hsc70-binding region of M1, a pull-down assay was performed using M1 deletion mutants (Fig. 2). M1ΔN lacked 2–75 aa; M1ΔM lacked 76–116 aa, including the NLS sequence;

Table 1
Primers used for the vector construction.

| Plasmid	Primer	Sequences
N384	Hsc70_1aa_F	5′-CCGGGATCCATGTCCAAGGGA-3′
	Hsc70_384aa_R	5′-CGGGGATCCCTTGTCTCCAGACAAGATGG-3′
N402	Hsc70_1aa_F	5′-CCGGGATCCATGTCCAAGGGA-3′
	Hsc70_402aa_R	5′-CGGGGATCCACCAAGGGAAAGAGGAGTG-3′
N462	792FH	5′-ATGGTCAACCATTTTATTGC-3′
	1470R	5′-CTGTGAGTTCAAACTTGCC-3′
N546	F4	5′-GGTGTTCCTCAGATTGAAGTC-3′
	1722R	5′-AGGCATAGGACTCAAGTGAA-3′
C385	Hsc70_385aa_F	5′-CGGGGATCCTCTGAGAATGTTCAAGATTTGCTG-3′
	Hsc70_END_R	5′-GGTGGATCCGATACTTGGTTG-3′
C403	Hsc70_403aa_F	5′-CGGGGATCCATTGAAACTGCTGGTGGAG-3′
	Hsc70_END_R	5′-GGTGGATCCGATACTTGGTTG-3′
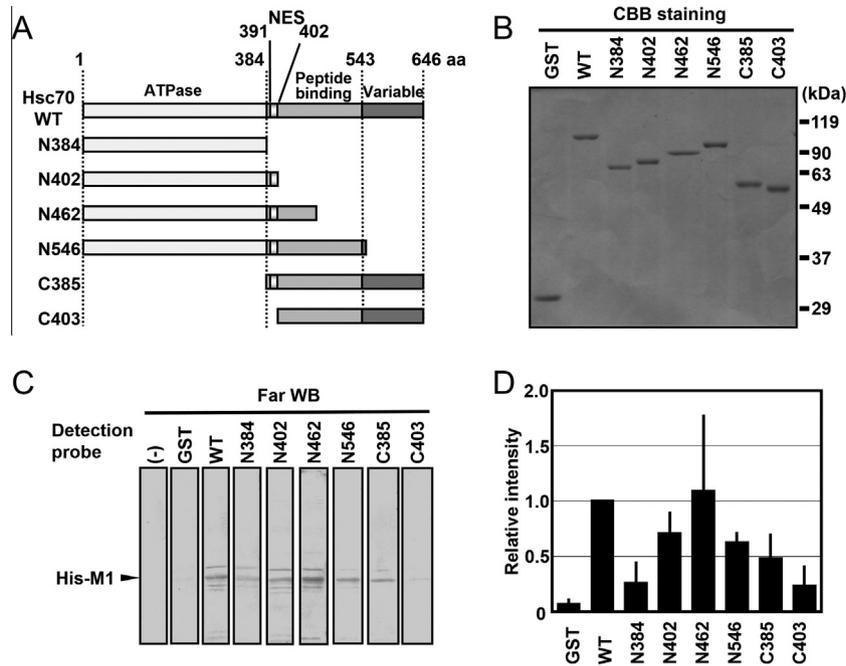
Fig. 1. Association of Hsc70 with M1 via the NES region in the N-terminal half of the peptide-binding domain. (A) Schematic representations of Hsc70 deletion mutants. (B) Purified GST-fused Hsc70 deletion mutants. One microgram-equivalent of the purified GST-fused Hsc70 mutants was loaded onto 10% SDS–PAGE, followed by CBB staining. (C) Far-western blotting assay. The far-western blotting assay was performed in accordance with a previously reported method [24]. In brief, the crude cell lysate of *E. coli* that expressed His–M1 was separated by 10% SDS–PAGE, transferred onto a PVDF membrane, and denatured with 6 M guanidine HCl in TBST for 10 min. After stepwise renaturating, the membrane was incubated without ["(−)"] or with 1 μg/mL of each purified GST or the series of GST–Hsc70 deletion mutants (see panels A and B). Specific signals were detected by western blotting using anti-GST antibody. Representative data from three independent experiments are shown. (D) The band intensity was measured using ImageJ software. Data represent the means and standard deviations from three independent experiments.

Table 2
Relative band intensities for Hsc70–M1 interaction.

Hsc70 mutants	Relative band intensities ± SD
GST	0.07 ± 0.05
Wild type	1
N384	0.26 ± 0.19
N402	0.71 ± 0.20
N462	1.09 ± 0.69
N546	0.63 ± 0.10
C385	0.48 ± 0.23
C403	0.23 ± 0.19

and M1ΔC lacked 112–252 aa (Fig. 2A). Recombinant His–M1s and GST–Hsc70 were purified and used for the *in vitro* pull-down assays. GST–Hsc70 was coprecipitated when His-bind resin-immobilized wild-type M1, ΔN, and ΔM were used (Fig. 2B: lanes 4, 6, and 8). No signal was detected when M1ΔC (lane 8) was used, suggesting that the C-terminal half of M1 is essential for Hsc70 binding.

3.3. K_d values for Hsc70–M1 binding and NS2–M1 binding

We previously reported Hsc70–M1 [24] and NS2–M1 binding [17] *in vitro*. In the present study, the binding of Hsc70–M1 and
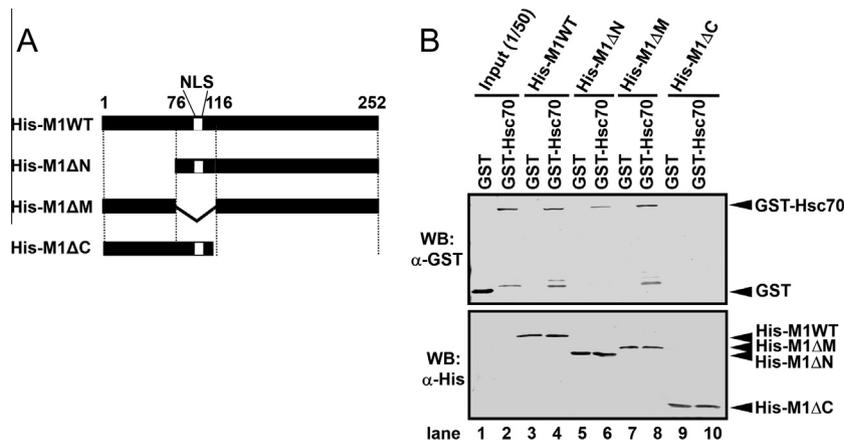

Fig. 2. Association of M1 with Hsc70 via the M1 C-terminal domain. (A) Schematic representations of the M1 deletion mutants. The nuclear localization signals (NLS, 101–105 aa) are indicated. (B) Results of the pull-down assays performed using His-tag-fused M1 deletion mutants and GST–NS2. The His-tag-fused M1 mutants (1.0 μg) on His-bind resin were incubated with 2.0 μg of GST or GST–NS2. To detect His–M1 and GST–NS2, a western blot analysis was performed using either anti-His (lower panel) or anti-GST (upper panel). In this assay, 1/50 of the total volume of His–M1 was loaded as the input (lanes 1 and 2) and 1/4 of the total volume of each eluted sample was loaded (lanes 3–10).

NS2–M1 was elucidated by Scatchard plot analysis (Fig. 3B). *In vitro* pull-down assays were performed using His–M1 and GST–NS2 or GST–Hsc70. The unbound and bound fractions were loaded onto SDS–PAGE, followed by western blotting. Each band was quantified and analyzed using ImageJ software. The K_d values for Hsc70–M1 and NS2–M1 binding were 1×10^{-7} M and 6×10^{-6} M, respectively. These results suggest that the binding of Hsc70–M1 is stronger than that of NS2–M1.

3.4. Hsc70 competes with NS2 for M1 binding

Next, to elucidate the binding modes of M1, NS2, and Hsc70, *in vitro* pull-down assays were performed (Fig. 4). The band intensity of GST–Hsc70 decreased when His–M1 and GST–Hsc70 were co-incubated with increasing amounts of GST–NS2, whereas that of GST–NS2 increased (Fig. 4A). Furthermore, the band intensity of GST–NS2 decreased when His–M1 and GST–NS2 were co-incubated with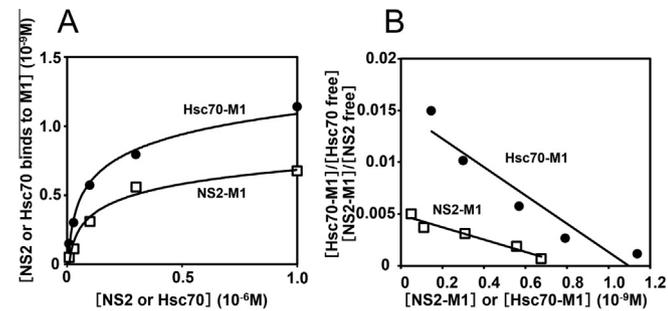 increasing amounts of GST–Hsc70, whereas that of GST–Hsc70 increased (Fig. 4B). These results suggest that Hsc70 competes with NS2 for M1 binding. To exclude the possibility that Hsc70 directly binds to NS2, GST pull-down assays were performed using GST–Hsc70 and His–M1 or His–NS2 (Fig. 4C). As expected, we confirmed the association between Hsc70 and M1, but no association between Hsc70 and NS2 was detected in our experimental conditions.

4. Discussion

In this study, we examined the binding of Hsc70 and NS2 to M1 based on biochemical analyses. We found that Hsc70 binds to M1 via its peptide-binding domain and characterized the K_d values of the Hsc70–M1 and NS2–M1 interactions.

The Scatchard plot analysis showed that the apparent K_d value of the Hsc70–M1 interaction was 1×10^{-7} M (Fig. 3). This is comparable to other reports for Hsc70-binding proteins. The anti-cell death protein, BAG-1, binds to Hsc70 as a monomer with a 1:1 stoichiometry (K_d value = 1×10^{-7} M) [29]. The interaction between Hsc70 and 1–20 aa of ribonuclease A has a K_d value of 2.7×10^{-6} M [30]. The N-terminal peptide of sickle cell hemoglobin binds to Hsc70 with a K_d value of 9.3×10^{-6} M [30]. It is unlikely that the ATPase activity of Hsc70 is involved in the Hsc70–M1 interaction because the addition of ATP did not affect the Hsc70–M1 binding (data not shown). We also determined the K_d value of the NS2–M1 interaction (6×10^{-6} M). These biochemical experiments help to elucidate the molecular mechanisms that facilitate the assembly of viral components. The interaction of Hsc70–M1 was stronger than that of NS2–M1, thereby suggesting an important role of Hsc70 in the export of vRNP.

It is well known that the nuclear export of vRNP is suppressed by LMB, suggesting that vRNP is exported via a CRM1-dependent pathway. Many studies suggest that M1 and NS2 are crucial for the nuclear export of vRNP, but the precise mechanism and structure of the nuclear export vRNP complex still remain controversial. We previously reported that Hsc70 is associated with vRNP–M1
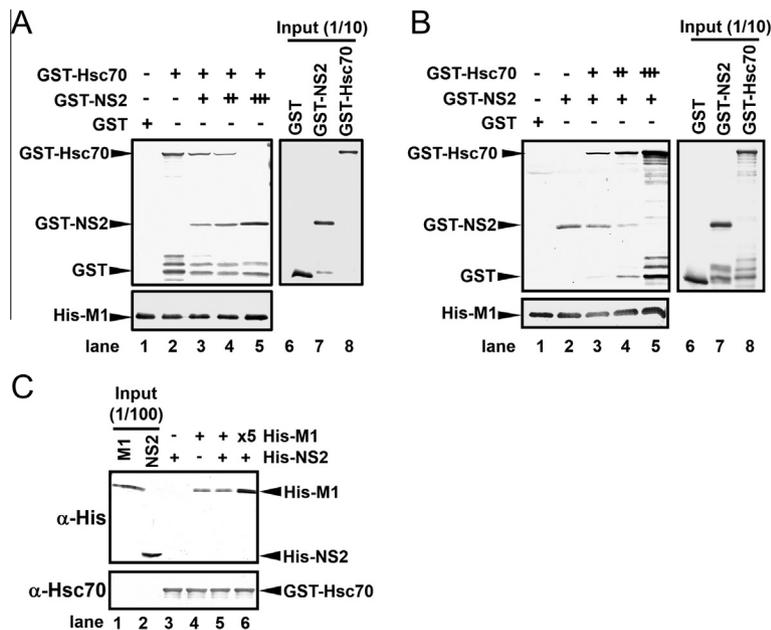

Fig. 3. Comparison of Hsc70–M1 and NS2–M1 binding. *In vitro* pull-down assays were performed using different concentrations of Hsc70 or NS2, as described in Materials and methods. (A) Saturation kinetics for Hsc70–M1 (closed circle) and NS2–M1 (open square) binding. (B) Scatchard plot analysis. Hsc70–M1 (closed circle) and NS2–M1 (open square) are shown.

Fig. 4. Hsc70 competes with NS2 for M1 binding. (A and B) Hsc70 and NS2 compete for M1 binding. His–M1 (2 μg) was immobilized on His-bind resin. In panel A, GST (lane 1), GST–Hsc70 (2.2 μg; lanes 2–5), and increasing amounts of GST–NS2 (2.7, 13.5, and 67.3 μg; lanes 3–5) were added to the reaction. In panel B, GST (lane 1), GST–NS2 (2.7 μg; lanes 2–5), and increasing amounts of GST–Hsc70 (2.2, 10.8, and 53.8 μg; lanes 3–5) were added to the reaction. To detect the GST-fused and His–M1 proteins, 1/4 of the volumes of the eluted pull-down samples were loaded onto SDS–PAGE, followed by detection with anti-GST and anti-His antibodies, respectively. (C) Hsc70 does not bind to NS2. *In vitro* pull-down assays were performed using GST–Hsc70 (0.5 μg; lanes 3–6) on glutathione Sepharose and His–NS2 (2.0 μg; lanes 3, 5, and 6) or His–M1 (2.0 μg; lanes 4 and 5, 10 μg; lane 6). In this assay, 1/100 of the total volumes of M1 and NS2 were loaded as the input (lanes 1 and 2).

complex [27]. It is unlikely that the vRNP–M1–Hsc70 complex contains NS2 because Hsc70 did not bind to NS2 directly (Fig. 4C), and it competed with NS2 for M1 binding (Fig. 4A and B). We detected no interaction between endogenous Hsc70 and recombinant NS2 when an infected cell lysate was used in the pull-down assay (data not shown). In addition, it has been reported that the replication of vRNP is regulated by M1 [31] and NS2 [32,33]. It was recently reported that NS2 is related to the adaptation of the highly pathogenic avian virus (H5N1) to a mammalian host [34]. It is likely that Hsc70 may affect these functions because the localization of Hsc70 drastically changed to the nucleus in the late stages of influenza viral infection, where M1 and NS2 were localized in the nucleus [14]. Hsc70 is constitutively expressed in influenza virus-susceptible cell lines, thereby suggesting the important roles of Hsc70 in influenza virus replication.

At present, two main classes of anti-influenza drugs are available: M2 ion channel inhibitors and NA inhibitors. The use of M2 ion channel inhibitors is limited by the rapid spread of drug-resistant influenza viruses, their side effects, and their limitation to influenza A virus [35]. Resistance to viral NA inhibitors is also increasing rapidly [36,37]. These factors necessitate the development of novel anti-influenza drugs with less likelihood of resistance emergence. Thus, the regulation of the functions of Hsc70 may lead to the development of new anti-influenza virus drugs. In conclusion, we demonstrated the presence of an interaction domain between M1 and Hsc70. In addition, we determined the K_d values of the Hsc70–M1 and NS2–M1 interactions. Considering previous analyses of Hsc70 in the viral life cycle, the regulation of the M1–NS2 interaction by Hsc70 could potentially be a good target for the development of anti-influenza viral drug. Further studies are ongoing to determine the detailed mechanism of vRNP export.

Funding

Conflict of interest

The authors have no conflict of interests to declare.

References

[1] Stegmann, T. (2000) Membrane fusion mechanisms: the influenza hemagglutinin paradigm and its implications for intracellular fusion. Traffic 1, 598–604.

[2] Herz, C., Stavnezer, E., Krug, R. and Gurney Jr., T. (1981) Influenza virus, an RNA virus, synthesizes its messenger RNA in the nucleus of infected cells. Cell 26, 391–400.

[3] Hutchinson, E.C. and Fodor, E. (2012) Nuclear import of the influenza A virus transcriptional machinery. Vaccine 30, 7353–7358.

[4] Momose, F., Kikuchi, Y., Komase, K. and Morikawa, Y. (2007) Visualization of microtubule-mediated transport of influenza viral progeny ribonucleoprotein. Microbes Infect. 9, 1422–1433.

[5] Kawaguchi, A., Matsumoto, K. and Nagata, K. (2012) YB-1 functions as a porter to lead influenza virus ribonucleoprotein complexes to microtubules. J. Virol. 86, 11086–11095.

[6] Rossman, J.S. and Lamb, R.A. (2011) Influenza virus assembly and budding. Virology 411, 229–236.

[7] Martin, K. and Helenius, A. (1991) Nuclear transport of influenza virus ribonucleoproteins: the viral matrix protein (M1) promotes export and inhibits import. Cell 67, 117–130.

[8] Bui, M., Wills, E.G., Helenius, A. and Whittaker, G.R. (2000) Role of the influenza virus M1 protein in nuclear export of viral ribonucleoproteins. J. Virol. 74, 1781–1786.

[9] Fornerod, M., Ohno, M., Yoshida, M. and Mattaj, I.W. (1997) CRM1 is an export receptor for leucine-rich nuclear export signals. Cell 90, 1051–1060.

[10] Iwatsuki-Horimoto, K., Horimoto, T., Fujii, Y. and Kawaoka, Y. (2004) Generation of influenza A virus NS2 (NEP) mutants with an altered nuclear export signal sequence. J. Virol. 78, 10149–10155.

[11] Huang, S., Chen, J., Chen, Q., Wang, H., Yao, Y., Chen, J. and Chen, Z. (2013) A second CRM1-dependent nuclear export signal in the influenza A virus NS2 protein contributes to the nuclear export of viral ribonucleoproteins. J. Virol. 87, 767–778.

[12] Cao, S., Liu, X., Yu, M., Li, J., Jia, X., Bi, Y., Sun, L., Gao, G.F. and Liu, W. (2012) A nuclear export signal in the matrix protein of Influenza A virus is required for efficient virus replication. J. Virol. 86, 4883–4891.

[13] Yu, M., Liu, X., Cao, S., Zhao, Z., Zhang, K., Xie, Q., Chen, C., Gao, S., Bi, Y., Sun, L., Ye, X., Gao, G.F. and Liu, W. (2012) Identification and characterization of three novel nuclear export signals in the influenza A virus nucleoprotein. J. Virol. 86, 4970–4980.

[14] Watanabe, K., Takizawa, N., Katoh, M., Hoshida, K., Kobayashi, N. and Nagata, K. (2001) Inhibition of nuclear export of ribonucleoprotein complexes of influenza virus by leptomycin B. Virus Res. 77, 31–42.

[15] Elton, D., Simpson-Holley, M., Archer, K., Medcalf, L., Hallam, R., McCauley, J. and Digard, P. (2001) Interaction of the influenza virus nucleoprotein with the cellular CRM1-mediated nuclear export pathway. J. Virol. 75, 408–419.

[16] Kudo, N., Matsumori, N., Taoka, H., Fujiwara, D., Schreiner, E.P., Wolff, B., Yoshida, M. and Horinouchi, S. (1999) Leptomycin B inactivates CRM1/exportin 1 by covalent modification at a cysteine residue in the central conserved region. Proc. Natl. Acad. Sci. U.S.A. 96, 9112–9117.

[17] Shimizu, T., Takizawa, N., Watanabe, K., Nagata, K. and Kobayashi, N. (2011) Crucial role of the influenza virus NS2 (NEP) C-terminal domain in M1 binding and nuclear export of vRNP. FEBS Lett. 585, 41–46.

[18] Yasuda, J., Nakada, S., Kato, A., Toyoda, T. and Ishihama, A. (1993) Molecular assembly of influenza virus: association of the NS2 protein with virion matrix. Virology 196, 249–255.

[19] Akarsu, H., Burmeister, W.P., Petosa, C., Petit, I., Muller, C.W., Ruigrok, R.W. and Baudin, F. (2003) Crystal structure of the M1 protein-binding domain of the influenza A virus nuclear export protein (NEP/NS2). EMBO J. 22, 4646–4655.

[20] O'Neill, R.E., Talon, J. and Palese, P. (1998) The influenza virus NEP (NS2 protein) mediates the nuclear export of viral ribonucleoproteins. EMBO J. 17, 288–296.

[21] Neumann, G., Hughes, M.T. and Kawaoka, Y. (2000) Influenza A virus NS2 protein mediates vRNP nuclear export through NES-independent interaction with hCRM1. EMBO J. 19, 6751–6758.

[22] Boulo, S., Akarsu, H., Ruigrok, R.W. and Baudin, F. (2007) Nuclear traffic of influenza virus proteins and ribonucleoprotein complexes. Virus Res. 124, 12–21.

[23] Ma, K., Roy, A.M. and Whittaker, G.R. (2001) Nuclear export of influenza virus ribonucleoproteins: identification of an export intermediate at the nuclear periphery. Virology 282, 215–220.

[24] Watanabe, K., Fuse, T., Asano, I., Tsukahara, F., Maru, Y., Nagata, K., Kitazato, K. and Kobayashi, N. (2006) Identification of Hsc70 as an influenza virus matrix protein (M1) binding factor involved in the virus life cycle. FEBS Lett. 580, 5785–5790.

[25] Perez-Vargas, J., Romero, P., Lopez, S. and Arias, C.F. (2006) The peptide-binding and ATPase domains of recombinant hsc70 are required to interact with rotavirus and reduce its infectivity. J. Virol. 80, 3322–3331.

[26] Tsukahara, F. and Maru, Y. (2004) Identification of novel nuclear export and nuclear localization-related signals in human heat shock cognate protein 70. J. Biol. Chem. 279, 8867–8872.

[27] Watanabe, K., Takizawa, N., Noda, S., Tsukahara, F., Maru, Y. and Kobayashi, N. (2008) Hsc70 regulates the nuclear export but not the import of influenza viral RNP: a possible target for the development of anti-influenza virus drugs. Drug Discov. Ther. 2, 77–84.

[28] Tsukahara, F., Yoshioka, T. and Muraki, T. (2000) Molecular and functional characterization of HSC54, a novel variant of human heat-shock cognate protein 70. Mol. Pharmacol. 58, 1257–1263.

[29] Stuart, J.K., Myszka, D.G., Joss, L., Mitchell, R.S., McDonald, S.M., Xie, Z., Takayama, S., Reed, J.C. and Ely, K.R. (1998) Characterization of interactions between the anti-apoptotic protein BAG-1 and Hsc70 molecular chaperones. J. Biol. Chem. 273, 22506–22514.

[30] Kwon, O.S. and Churchich, J.E. (1994) Interaction of 70-kDA heat shock cognate protein with peptides and myo-inositol monophosphatase. J. Biol. Chem. 269, 266–271.

[31] Ye, Z.P., Baylor, N.W. and Wagner, R.R. (1989) Transcription-inhibition and RNA-binding domains of influenza A virus matrix protein mapped with anti-idiotypic antibodies and synthetic peptides. J. Virol. 63, 3586–3594.

[32] Robb, N.C., Smith, M., Vreede, F.T. and Fodor, E. (2009) NS2/NEP protein regulates transcription and replication of the influenza virus RNA genome. J. Gen. Virol. 90, 1398–1407.

[33] Odagiri, T. and Tobita, K. (1990) Mutation in NS2, a nonstructural protein of influenza A virus, extragenically causes aberrant replication and expression of the PA gene and leads to generation of defective interfering particles. Proc. Natl. Acad. Sci. U.S.A. 87, 5988–5992.

[34] Manz, B., Brunotte, L., Reuther, P. and Schwemmle, M. (2012) Adaptive mutations in NEP compensate for defective H5N1 RNA replication in cultured human cells. Nat. Commun. 3, 802.

[35] Hayden, F.G. (2006) Antiviral resistance in influenza viruses – implications for management and pandemic response. N. Engl. J. Med. 354, 785–788.

K. Watanabe et al. / FEBS Open Bio 4 (2014) 683–688

[36] Stephenson, I., Democratis, J., Lackenby, A., McNally, T., Smith, J., Pareek, M., Ellis, J., Bermingham, A., Nicholson, K. and Zambon, M. (2009) Neuraminidase inhibitor resistance after oseltamivir treatment of acute influenza A and B in children. Clin. Infect. Dis. 48, 389–396.

[37] Kiso, M., Mitamura, K., Sakai-Tagawa, Y., Shiraishi, K., Kawakami, C., Kimura, K., Hayden, F.G., Sugaya, N. and Kawaoka, Y. (2004) Resistant influenza A viruses in children treated with oseltamivir: descriptive study. Lancet 364, 759–765.